Characterization of a spontaneously immortalized murine Müller glial cell line QMMuC-1

Augustine, J., Pavlou, S., O'Hare, M., Harkin, K., Stitt, A., Curtis, T., ... Chen, M. (2018). Characterization of a spontaneously immortalized murine Müller glial cell line QMMuC-1. Investigative Opthalmology and Visual Science, 59(3), 1666-1674. DOI: 10.1167/iovs.17-23293

Published in:
Investigative Opthalmology and Visual Science

Document Version:
Publisher's PDF, also known as Version of record

Queen's University Belfast - Research Portal:
Link to publication record in Queen's University Belfast Research Portal

Characterization of a Spontaneously Immortalized Murine Müller Glial Cell Line QMMuC-1

Josy Augustine, Sofia Pavlou, Michael O'Hare, Kevin Harkin, Alan Stitt, Tim Curtis, Heping Xu, and Mei Chen

Wellcome-Wolfson Institute for Experimental Medicine, Queen's University Belfast, Northern Ireland, United Kingdom

Correspondence: Mei Chen, Wellcome-Wolfson Institute for Experimental Medicine, Queen's University Belfast, Northern Ireland, UK; m.chen@qub.ac.uk.

JA and SP contributed equally to the work presented here and should therefore be regarded as equivalent authors.

Submitted: November 3, 2017
Accepted: February 13, 2018

Citation: Augustine J, Pavlou S, O'Hare M, et al. Characterization of a spontaneously immortalized murine Müller glial cell line QMMuC-1. *Invest Ophthalmol Vis Sci*. 2018;59:1666–1674. https://doi.org/10.1167/iovs.17-23293

Purpose. Müller glia are critical for the survival of retinal neurons and the integrity of retinal blood vessels. Müller glial cultures are important tools for investigating Müller glial pathophysiology. Here, we report a spontaneously immortalized Müller glial cell line originally cultured and subsequently cloned from mouse pups. The cell line, Queen's University Murine Müller glia Clone-1 (QMMuC-1), has been cultured for over 60 passages, has morphologic features like primary Müller cell (PMC) cultures and remains stable.

Methods. QMMuC-1 and PMC cells were processed for immunohistochemistry, quantitative RT-PCR, Western blotting, whole cell voltage-clamping, and bioenergetic profiling.

Results. Immunocytochemistry showed that QMMuC-1 express known Müller glial markers, including glutamine synthetase, glial fibrillary acidic protein (GFAP), alpha-smooth muscle actin (α-SMA), Aquaporin 4, Kir4.1, interleukin 33 (IL-33), and sex determining region Y (SRY)-box2 (Sox2), but not Cone arrestin, Calbindin 1, CD68, and ionized calcium-binding adapter molecule 1 (Iba1). Compared with PMC, QMMuC-1 express higher levels of chemokine (C-C motif) ligand 2 (Ccl2), VEGFA, and glutamate aspartate transporter (GLAST), but lower levels of interleukin 6 (IL-6), brain-derived neurotrophic factor (BDNF), insulin-like growth factor 1 (IGF1), and neurotrophin 3 (NTF3). Whole-cell patch clamp recordings demonstrated characteristic inward currents in response to L-glutamate and L-trans-pyrrolidine-2,4-dicarboxylic acid (PDC) by QMMuC-1 cells. The L-glutamate–induced current was significantly higher in QMMuC-1 cells compared with PMC. Bioenergetic profiling studies revealed similar levels of glycolysis and basal mitochondrial respiration between QMMuC-1 and PMC. However, mitochondrial spare capacity was significantly lower in QMMuC-1 compared with PMC.

Conclusions. Our results suggest that the QMMuC-1 Müller glial cell line retains key characteristics of PMC with its unique profiles in cytokine/neurotrophic factor expression and mitochondrial respiration. QMMuC-1 has utility as an invaluable tool for understanding the role of Müller glia in physiological and pathological conditions.

Keywords: Müller glia, cell line, cytokines, glycolysis, mitochondrial respiration, glutamate, physiological response

Multiple cell types contribute to the neurovascular unit in the retina, including neurons, macroglial elements (astrocytes and Müller glia), vascular cells (endothelia and pericytes), and associated immune cells (microglia).[1] Müller glia represent the main glial population of the retina and play a key role in maintaining the retinal architecture.[2] Although their morphology differs between species, Müller glia do have some common features. The nuclei of Müller glia, for example, are consistently located within the inner nuclear layer of the retina and their cell bodies stretch in opposite directions extending from the outer to the inner limiting membranes.

Müller glia have a range of functions and are vital for neuronal survival and the maintenance of the inner blood–retinal barrier.[2,3] They play a critical role in regulating retinal cell metabolism and ion (mainly K^+) and water homeostasis in the extracellular space.[4] Müller glia continuously uptake and metabolize neurotransmitters, such as glutamate,[5] and thus are important in supporting synaptic activity and preventing excitotoxicity. Müller glia release various neurotrophic factors and contribute to cell survival and axonal growth.[2] They can also act as light guides, serving to direct incoming light to photoreceptor cells.[6,7] In some species, Müller glia display some features of retinal stem cells. For instance, in response to acute retinal damage, Müller glia from fish and adult birds may re-enter the mitotic cycle, proliferate, and de-differentiate into neurons.[8,9] In mammals, they can proliferate and express genes that are associated with retinal stem cells,[10–12] but do not appear to function as retinal progenitors in vivo.[13]

Müller glial cultures have made a significant contribution for understanding retinal pathophysiology, especially in the context of retinal degenerative diseases. Primary Müller glial cultures have several advantages, largely due to their phenotypic and functional similarity to Müller glia in vivo. There are, however, several disadvantages in using primary cultures, including limited availability, and inconsistency in experimental results, perhaps due to purity, heterogeneity across different batches, and phenotypic instability across multiple passages.[14] The use of a stabilized cell line can overcome these drawbacks, although it is recommended that key results obtained from cell lines are further validated using primary cells and in vivo models. Various

Table 1. Primary Antibodies Used for Immunofluorescence

Antibody	Dilution	Company	Catalog Number
Aqp4	1:200	Santa Cruz (Dallas, TX, USA)	SC-20812
α-SMA	1:200	Sigma-Aldrich	091M4815
CD68	1:300	BioRad	MCA1957
Cone arrestin	1:1000	Millipore (Darmstadt, Germany)	AB15282
Cralbp	1:200	Abcam (Cambridge, UK)	AB15051
eNOS	1:200	BD Biosciences (Franklin Lakes, NJ, USA)	610297
FGFR4	1:50	Proteintech (Chicago, IL, USA)	11098-1-AP
GFAP	1:200	Abcam	Ab16997-1
GS	1:2000	Sigma-Aldrich	G2781
Iba1	1:100	WAKO (Osaka, Japan)	019741
IL-33	1:50	R&D (Minneapolis, MN, USA)	AF3626
Kir4.1	1:200	Abcam	AB105102
Sox2	1:200	Abcam	AB97959
Vim	1:100	Biorbyt (Cambridge, UK)	ORB167196

Müller glial cell lines, derived from rodents[14–17] or humans[18] have been reported. Although they all express Müller glial markers, each cell line has its own characteristics and is used to study different functions of Müller glia. For example, MIO-M1 cells express neural progenitor genes such as SRY (sex determining region Y)-box 2 (*Sox2*), paired box 6 (*Pax6*), and *Notch 1*.[11] They can form neurospheres when grown in the presence of an extracellular matrix and fibroblast growth factor-2.[11] These cells are therefore a useful tool for studying Müller glial reprogramming and progenitor functions. The rMC-1 cells were generated from intense light exposed retinas of Sprague-Dawley rats.[14] These cells strongly express glial fibrillary acidic protein (GFAP), which may reflect the reactive gliosis induced by light damage. These cells, however, express high levels of serine racemase and alanine, serine, cysteine transporter 2 (ASCT-2), and thus, are a useful tool for studying the role of Müller glia in regulating N-methyl-D-aspartate (NMDA) receptors in adjacent neurons.[19] The ImM10 cell line is a conditionally immortalized Müller glial cell line from *H-2K^b-tsA58/+;HRhoGFP/+* mice.[15] These cells, like MIO-M1 cells, express retinal stem cell genes and can form neurospheres in sphere-forming conditions,[20] and therefore, are most suitable for studying the progenitor behaviors of Müller cells. Herein, we report a newly established Müller cell line derived from murine retina, which we have called Queen's University Murine Müller glia Clone-1 (QMMuC-1). QMMuC-1 retain Müller glial morphology after 60 passages in vitro, while maintaining phenotypic features and electrophysiological characteristics, analogous to those observed in primary Müller glia.[21] This new cell line provides an important platform for furthering our understanding of Müller glial function in both retinal health and disease.

Materials and Methods

Müller Glial Culture

Primary Müller cells (PMC) were isolated from C57BL/6J neonatal mice (P7) and were cultured using a protocol described previously.[22,23] Cells were grown in Dulbecco's Modified Eagle Media (DMEM; Thermo Fisher Scientific, Waltham, MA, USA) containing 10% fetal calf serum (FCS) supplemented with 1% penicillin/streptomycin and 5% splenocyte-conditioned media. Splenocyte conditioned media were prepared by treating rat splenocytes with 2 μg/mL Concanavalin A (Sigma-Aldrich, Dorset, UK) for 18 hours, followed by methyl a-D-mannopyranoside (Sigma-Aldrich) for 30 minutes. One of the cultures had accelerated growth after passage 20 and was further cloned by limiting dilution using a 96-well plate. Ten wells with a single cell were noted 2 hours after plating. These wells were marked and selected for colony expansion. Five clones were obtained, and among them, clone 1, named QMMuC-1, was chosen for further characterization. PCR analysis using primer sets of mouse *β-globin*, rat *β-globin*, and rat *actin* confirmed mouse origin of the QMMuC-1 cells (data not shown).

QMMuC-1 cells were routinely cultured in a T75 flask in DMEM with 10% FCS and passaged at 1:4 every 3 days. The cell line has been maintained in the laboratory for over 10 months (>60 passages). QMMuC-1 did not show any abnormal growth changes after being thawed from liquid nitrogen.

Immunofluorescence (IF) Staining

IF staining was carried out as previously described.[24] Briefly, fixed cells were permeabilized with 0.1% Triton X-100 for 12 minutes and blocked in 1% BSA for 1 hour at room temperature. The samples were then incubated with primary antibodies (Table 1) overnight at 4°C. After thorough washes with PBS, the samples were incubated with an appropriate fluorophore conjugated secondary antibody (1:300) for 1 hour at room temperature. Cells were mounted using Vectashield medium-containing DAPI (Vector Laboratories, Brulingame, CA, USA) and examined using a C1 Nikon Eclipse TE200-U (Nikon, Surry, UK) or Olympus IX51 inverted fluorescent microscope (Olympus, Southend, UK). Images were processed using Fiji software (provided in the public domain, https://imagej.net/Fiji/).[25]

Growth Curve

The growth curve of QMMuC-1 cells was determined by seeding the cells at a density of 1000 cells/well in a 96-well microplate with DMEM and 10% FCS. The number of cells in 6 wells was counted every 24 hours for 7 days using a hemocytometer and the average number was used to calculate the doubling time and plot the growth curve, as previously described.[24]

Reverse Transcriptase Polymerase Chain Reaction (RT-PCR)

Total RNA was extracted using RNeasy Mini Kit (Qiagen, Hilden, Germany) and transcribed into cDNA using SuperScript II Reverse Transcriptase Kit (Thermo Fisher Scientific), according to the manufacturer's instructions. Validated TaqMan probes were purchased from Roche (Basel, Switzerland): IL-6 (300699), chemokine (C-C motif) ligand 2 (Ccl2; 310467), VEGFA (314944), TGFB1 (317139), and B-actin (307903). SYBR Green gene specific primers were designed using National Center for Biotechnology Information (NCBI) Primer Blast and synthesized by Integrated DNA Technologies (Coralville, IA, USA; Table 2). Quantitative RT-PCR was performed using a Roche LightCycler 480 real-time PCR machine. Relative gene expression was calculated using the comparative Ct method with data normalized to B-actin.

Western Blotting

Müller glia were homogenized in RIPA buffer supplemented with 10% proteinase inhibitor cocktail (Sigma-Aldrich) and

Table 2. SYBR Green Primer Sequences

Genes	Forward	Reverse
CNTF	AGCCTTGACTCAGTGGATGG	TGGAGGTTCTCTTGGAGTCG
BDNF	GGGTCACAGCGGCAGATAAA	GCCTTTGGATACCGGGACTT
GS	TGCCTGCCCAGTGGGAATT	TATTGGAAGGGTTCGTCGCC
GFAP	TGCAAGAGACAGAGGAGTGG	GCTCTAGGGACTCGTTCGTG
GLAST	CTCTGGGCATCCTCTTCTG	CAAATCTGGTGATGCGTTTG
Igf1	AGACAGCATTGTGGATGAG	TGAGTCTTGGGCATGTCAGT
Ntf3	AGGTGATGTCCATCTTGTTTT	GCCTCTCCCTGCTCTGGTTC
B-actin	CCTTCCTTCTTGGGTATG	TGTAAAACGCAGCTCAGTAA

protein concentration was determined using a BCA assay kit (Thermo-Fisher Scientific). Polyacrylamide gel of 12% was used and 50 μg of protein were loaded per lane. Proteins were transferred onto polyvinylidene fluoride (PVDF) membranes, blocked for 1 hour in 5% milk in PBS supplemented with 0.1% Tween 20, before being incubated with a primary antibody overnight at 4°C (Table 3). After several washes, membranes were incubated with suitable horseradish peroxidase (HRP) conjugated secondary antibodies (1:5000) for 1 hour at room temperature. Membranes were visualized with enhanced chemiluminescence (Clarity Western ECL Blotting Substrates; BioRad, Hercules, CA, USA) and bands detected using Syngene G-Box imaging system (Syngene, Cambridge, UK).

Bioenergetic Profile

Müller glial glycolytic function was measured using a Seahorse XF Glycolysis Stress Test Kit with a Seahorse XFe96 Analyzer (Agilent Technologies, Santa Clara, CA, USA).[26] QMMuC-1 and PMC were seeded at a density of 2000 cells per well onto a 96-well microplate (Agilent Technologies) 24 hours prior to the assay. Glycolytic activities were assessed by measuring the extracellular acidification rates (ECAR). Nonglycolytic acidification is defined as the ECAR before the addition of glucose. The increase in ECAR after glucose addition relates to the level of glycolysis. Glycolytic capacity is the maximum ECAR observed after the addition of oligomycin (2 μM) minus the nonglycolytic acidification. Mitochondrial function was assessed by directly measuring the oxygen consumption rates (OCR) using Seahorse XF Mito Stress Test kit. Basal respiration is defined as the basal OCR minus the OCR after the addition of antimycin A and rotenone, which represents nonmitochondrial respiration. ATP production is calculated by subtracting the OCR after the addition of oligomycin from the basal respiration. Proton leak is the OCR after oligomycin minus nonmitochondrial respiration. Maximal respiration is the maximum OCR achieved after the addition of Carbonyl cyanide-4-(trifluoromethoxy) phenylhydrazone (FCCP; 5 μM) minus nonmitochondrial respiration. The spare capacity is the difference between maximal and basal respiration. At the end of the experiment, cells were fixed, permeabilized, and stained with YOPRO-1. Their fluorescence intensity (arbitrary unit [AU]) was used to normalize the data.

Table 3. Antibodies Used for Western Blotting

Antibody	Dilution	Company	Catalog Number
Aqp4	1:500	Santa Cruz	SC-20812
B-actin	1:5000	Cell Signaling Technology (Danvers, MA, USA)	3700S
GFAP	1:800	Abcam	Ab16997-1
Kir4.1	1:500	Abcam	AB105102

Electrophysiology

Membrane currents were recorded using the whole cell voltage-clamp technique, using an Axopatch 200B amplifier (Axon Instruments, Foster City, CA, USA), and digitized with an analog-to-digital converter (Digidata 1322; Axon Instruments). pCLAMP software was used for data acquisition and analysis (version 9; Axon Instruments). Pipette resistances were 2 to 5 MΩ. Whole-cell currents were elicited using voltage ramp protocols from −80 to +20 mV applied over 625 ms from a holding potential of 0 mV.

Glutamate aspartate transporter (GLAST) currents were evoked by exposing the cells to L-glutamate (1 mM) and L-trans-pyrrolidine-2,4-dicarboxylic acid (PDC) (100 μM), respectively.[5,21] Current responses at −80 mV were measured by subtracting the baseline current from the maximum recorded current response during drug application. The bathing solution comprised 140 mM NaCl, 3 mM KCl, 1.8 mM $CaCl_2$, 0.8 mM $MgCl_2$, 3 mM $BaCl_2$, 10 mM Na-HEPES, and 5 mM glucose at pH 7.4. Barium was included in the bathing medium to block the cells' inward rectifier potassium channels. The pipette solution consisted of 50 mM KCl, 65 mM K_2SO_4, 6 mM $MgCl_2$, and 10 mM K-HEPES at pH 7.4.

Statistical Analysis

Data are presented as mean ± SEM. Statistical analysis was performed using unpaired, two-tailed Student's *t*-test. Welch's correction was used when the equal variance assumption was not met. Paired, two-tailed Student's *t*-test was used to analyze the electrophysiology data. $P < 0.05$ was considered statistically significant.

Results

Establishment of a Murine Müller Glial Cell Line

Using the culture protocol described above, PMC were routinely cultured from day 7 mouse pups. PMC displayed a flattened, elongated shape with multiple lamellipodia (Fig. 1A). These cells were positive for several Müller glial markers, such as GFAP, glutamine synthetase (GS), cellular retinaldehyde binding protein (CRALBP), Sox2, and IL-33 (Figs. 1B–F), but were negative for markers of other retinal cells including cone arrestin (cone photoreceptors), calbindin 1 (Calb1; amacrine cells), endothelial nitric oxide synthase (eNOS; vascular endothelial cells), fibroblast growth factor receptor 4 (FGFR4; fibroblasts), cluster of differentiation 68 (CD68, microglial cells), and ionized calcium-binding adapter molecule 1 (Iba1; microglial cells; Figs. 1G–L). These antibodies were tested in other tissues and cells and the negative staining of these antigens in our Müller cell cultures was not due to poor quality of reagents.

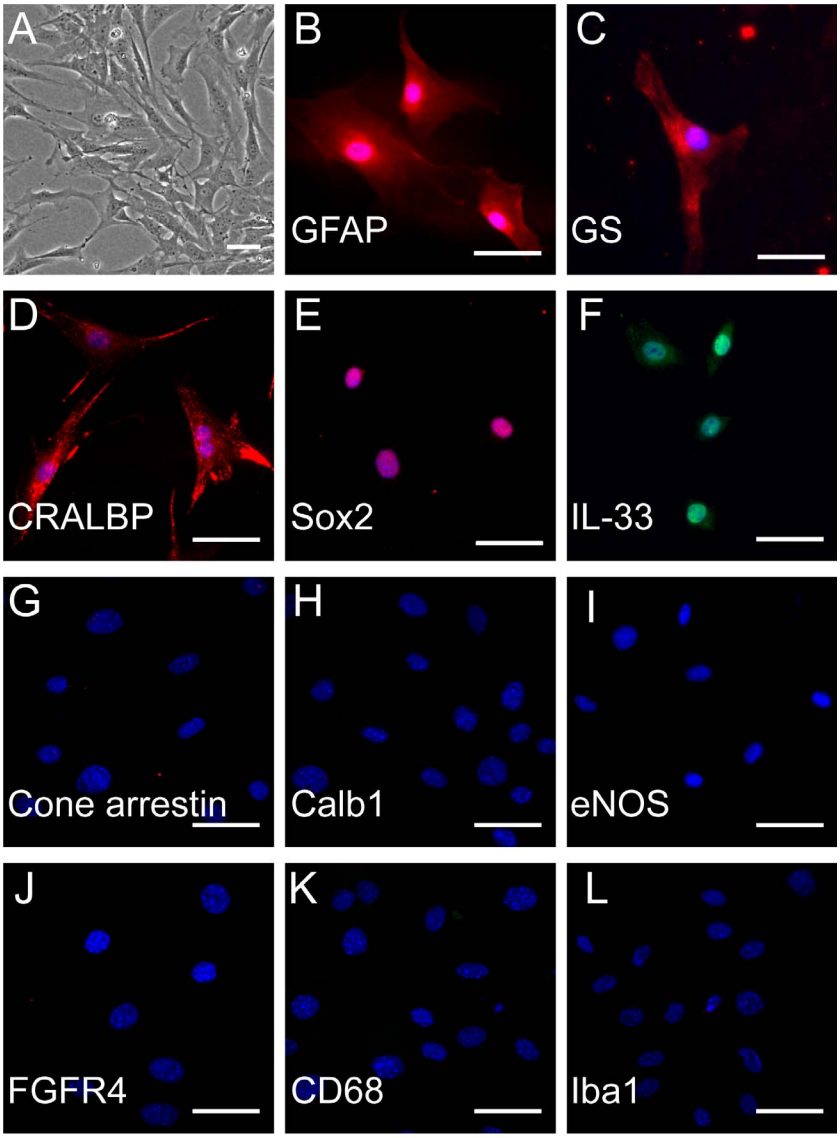

Figure 1. Characterization of PMC. (**A**) Flattened cell shape of PMC observed under light microscope. PMC are positive for (**B**) GFAP (*red*), (**C**) GS (*red*), (**D**) CRALBP (*red*), (**E**) Sox2 (*red*), (**F**) IL-33 (*green*), and negative for (**G**) Cone arrestin, (**H**) Calb1, (**I**) eNOS, (**J**) FGFR4, (**K**) CD68, and (**L**) Iba1. DAPI in *blue*. *Scale bar*: 50 μM.

During the primary Müller cell culture, one cell line was spontaneously immortalized and had been maintained in vitro for over 60 passages. The cell line was cloned and named as QMMuC-1 and further investigated. The morphology of QMMuC-1 (Fig. 2A) resembled that of PMC (Fig. 1A). The QMMuC-1 cells grew steadily under standard culture conditions and had a doubling time of 27.63 hours (Fig. 2B). The growth curve reached plateau at day 6 and QMMuC-1 cells form stable monolayers that can be maintained for prolonged periods of time.

IF staining showed that QMMuC-1 cells express known Müller glial markers, including GFAP, GS, CRALBP, Vimentin (Vim), potassium voltage-gated channel subfamily J member 10 (Kcnj10, also known as Kir4.1), Aquaporin 4 (Aqp4), alpha-smooth muscle actin (α-SMA), Sox2, and IL-33 (Figs. 2C–K). Aqp4, Sox2, and IL-33 displayed nuclear staining, whereas, other antigens were detected in the cytoplasm. The expression of GFAP, Kir4.1, and Aqp4 was further confirmed by Western blotting (Fig. 2L).

The Expression of Cytokines and Neuroprotective Factors by QMMuC-1

Müller glia release cytokines and neurotropic factors that are important for retinal homeostasis. RT-PCR analysis showed that both PMC and QMMuC-1 express Ccl2, IL-6, VEGFA, and TGFB1 under normal culture conditions (Figs. 3A–D). QMMuC-1 expressed higher levels of VEGFA and Ccl2 ($P < 0.01$), but lower levels of IL-6 ($P < 0.01$) and TGFB1 ($P < 0.05$) in comparison to PMC.

The neurotrophic factors ciliary neurotrophic factor (CNTF), brain-derived neurotrophic factor (BDNF), and insulin-like growth factor 1 (IGF1) were also detected in QMMuC-1 and PMC, with the expression of BDNF and IGF1 appearing significantly lower in QMMuC-1 cells as compared with PMC (Figs. 3E–G). In contrast to PMC, neurotrophin 3 (NTF3) was not detected in QMMuC-1 cells (Fig. 3H).

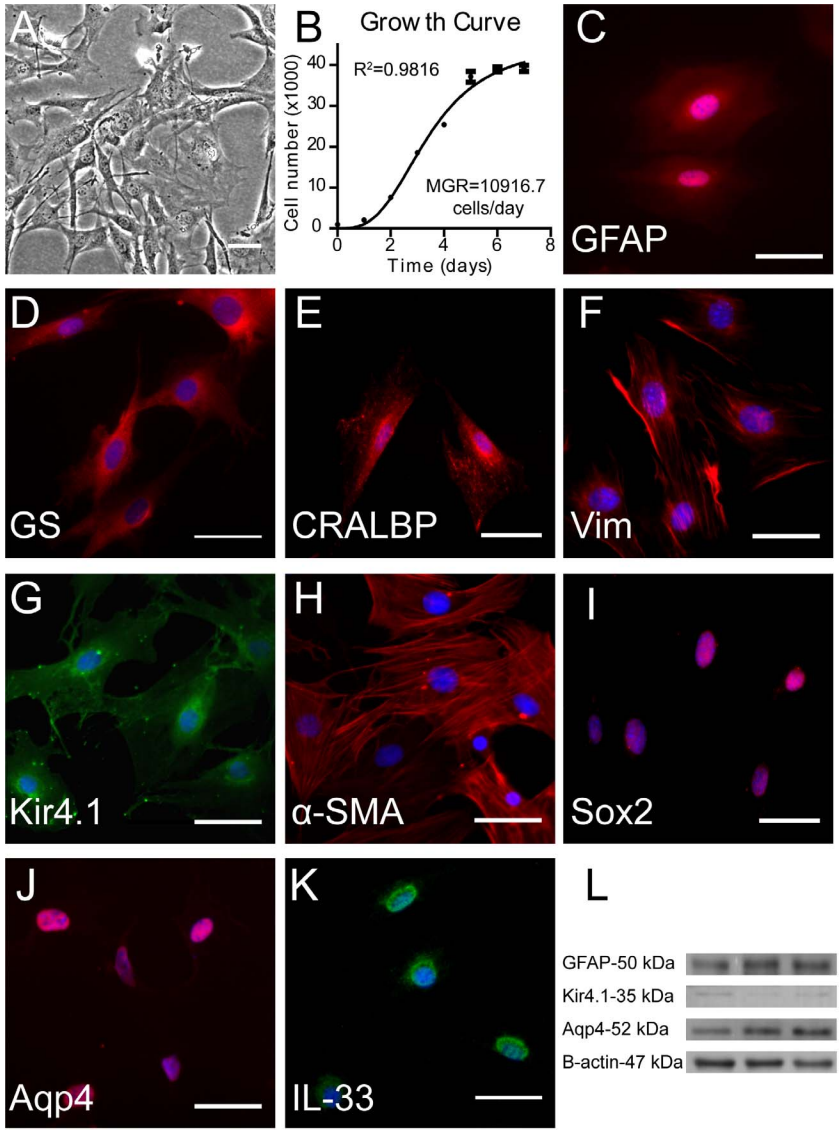

Figure 2. Characterization of QMMuC-1. (**A**) Morphology of QMMuC-1 observed under light microscope. (**B**) Growth curve for QMMuC-1 calculated by cell counting daily for 7 days. QMMuC-1 are positive for (**C**) GFAP (*red*), (**D**) GS (*red*), (**E**) CRALBP (*red*), (**F**) Vim (*red*), (**G**) Kir4.1 (*green*), (**H**) α-SMA (*red*), (**I**) Sox2 (*red*), (**J**) Aqp4 (*red*), and (**K**) IL-33 (*green*). DAPI in *blue*. *Scale bar*: 50 μm. (**L**) QMMuC-1 lysates were analyzed by Western blot for key Müller cell markers, GFAP, Kir4.1, Aqp4. B-actin was used as loading control. MGR, maximum growth rate.

GFAP is upregulated in activated Müller cells in vivo. QMMuC-1 express significantly lower levels of GFAP when compared with PMC ($P < 0.05$; Fig. 3I).

Electrophysiological Response to Glutamate

Müller glia play an important role in regulating glutamate levels in the retinal extracellular space.[5] They express electrogenic glutamate transporters, such as GLAST, to uptake and transport glutamate into the cytosol and then use GS to metabolize it into glutamine. Both GLAST and GS were detected in QMMuC-1 cells (Figs. 4A, 4B). The expression levels of GLAST were significantly higher in QMMuC-1 compared with PMC ($P < 0.01$). GS was also higher in QMMuC-1 compared with PMC, although the difference was not statistically significant. We subsequently used the whole-cell configuration of the patch-clamp technique to investigate whether QMMuC-1 cells display glutamate-induced currents. Application of L-glutamate to QMMuC-1 cells during voltage ramp protocols elicited inward (negative) currents that became progressively smaller as the cells were depolarized toward +20 mV (Figs. 4C, 4D). Glutamate not only increases the activity of the GLAST, but can also activate ionotropic glutamate receptors and block barium-insensitive outward currents in Müller glia.[27,28] Therefore, to specifically examine glutamate transporter currents, we tested the effects of the selective glutamate transporter ligand, PDC.[29] Consistent with the activation of GLAST, an increase in inward current was observed in QMMuC-1 cells during exposure to PDC (Figs. 4E, 4F). Similar responses to glutamate and PDC were observed in PMC. The glutamate-induced current was significantly higher in QMMuC-1 cells compared with PMC (Fig. 4G). PDC-induced current densities, however, were comparable between QMMuC-1 and PMC cells (Fig. 4H).

Bioenergetic Profile of QMMuC-1 Cells

Energy in the form of ATP and metabolic biomaterials are essential for cells to maintain homeostasis and specialized

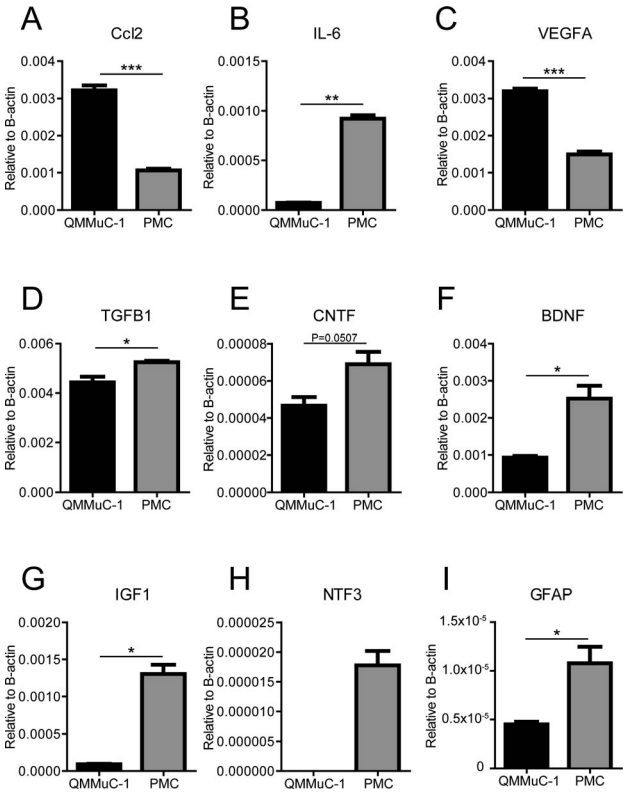

Figure 3. mRNA expression of cytokines and neuroprotective factors in QMMuC-1 and PMC. (**A**) Ccl2, (**B**) IL-6, (**C**) VEGFA, (**D**) TGFB1, (**E**) CNTF, (**F**) BDNF, (**G**) IGF1, (**H**) NTF3, and (**I**) GFAP mRNA expression was assessed by RT-PCR ($N = 3$). *Error bars* represent ± SEM (*$P <$ 0.05, **$P < 0.01$, ***$P < 0.001$).

functions. The major metabolic pathways including glycolysis and mitochondrial respiration were examined using the Seahorse XFe96 Analyzer system. The Glycolysis Stress Test assay showed that QMMuC-1 and PMC have similar nonglycolytic acidification rates (Figs. 5A, 5B). Upon addition of glucose, ECAR increased in both cell types followed by a further increase after inhibition of mitochondrial ATP synthesis using oligomycin (Fig. 5A). The rate of nonglycolytic acidification, glycolysis, and glycolytic capacity were comparable between QMMuC-1 and PMC (Fig. 5B–D).

Mitochondrial oxidative phosphorylation was tested using the Cell Mito Stress Test system (Figs. 5E–M). Both QMMuC-1 and PMC had similar levels of basal respiration, ATP production, proton leakage, and nonmitochondrial respiration (Figs. 5F, 5G, 5J, 5K). However, the maximal respiratory capacity and spare respiratory capacity were lower in QMMuC-1 cells compared with PMC (Figs. 5H, 5I). These results suggest that QMMuC-1 have a lower capacity to employ mitochondrial respiration under stressed conditions requiring extra energy.

To gain further insight into the relative utilization of mitochondrial respiration and glycolysis by Müller glia, we extracted and plotted OCR versus ECAR under basal and maximal respiration (after oligomycin and FCCP treatment) conditions from the Cell Mito Stress assay (Fig. 5L). Under basal conditions, the OCR/ECAR ratio was 4.79 ± 0.49 in QMMuC-1 cells and 2.85 ± 0.3 in PMC (Fig. 5L), suggesting that QMMuC-1 is predominately fueled by oxidative phosphorylation to maintain basal functions. After oligomycin and FCCP treatment, the PMC had significantly higher levels of response in both OCR and ECAR than QMMuC-1 cells (Fig. 5L), further

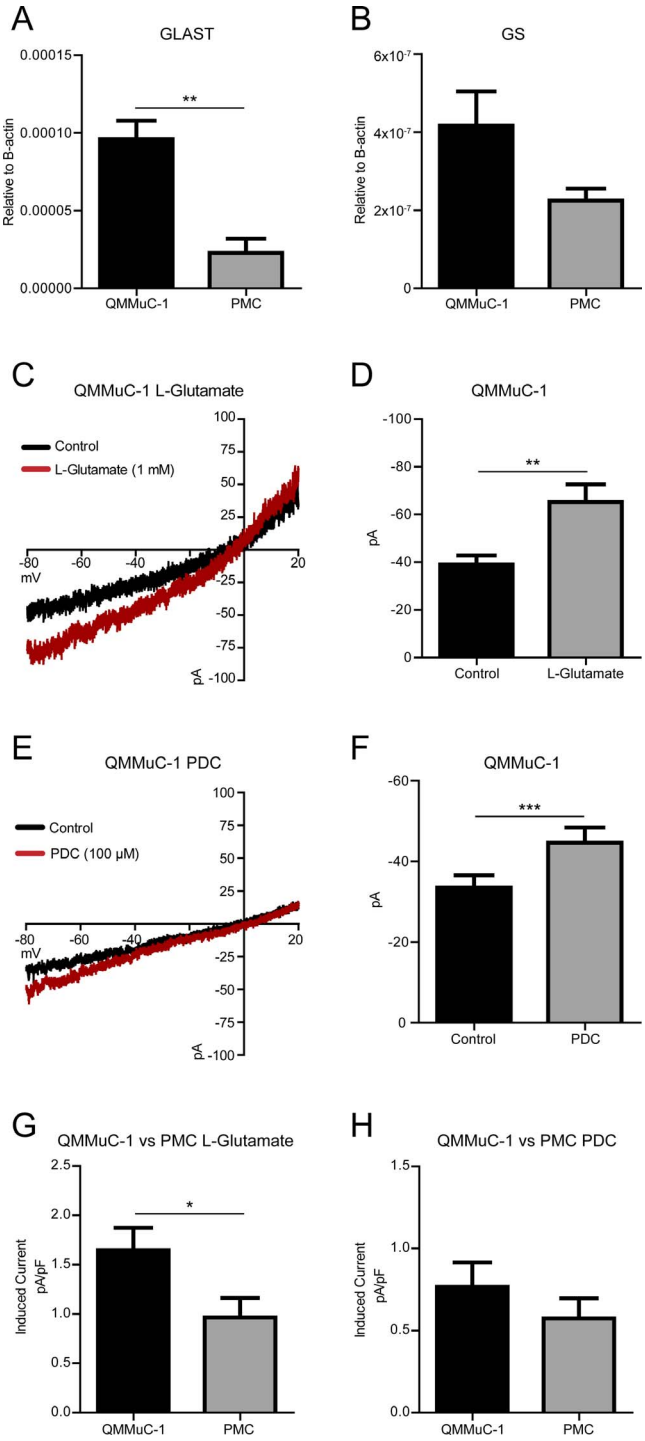

Figure 4. Whole-cell recordings of QMMuC-1 reveal characteristic responses to glutamate and PDC. (**A**) GLAST and (**B**) GS mRNA expression was assessed by RT-PCR. *Error bars* represent ± SEM. $N =$ 5. (**C**) Currents recorded using voltage ramp protocols prior to (*black*) and during L-Glutamate exposure (*red*). (**D**) Mean data showing peak currents before and after the application of L-Glutamate ($N = 7$). (**E**) Equivalent traces and (**F**) pooled data from QMMuC-1 cells exposed to PDC ($N = 8$). (**G**, **H**) Comparison of induced currents from QMMuC-1 and primary Müller cells during L-Glutamate (**G**, $N = 6$) and PDC (**H**, N $= 5$) exposure. *Error bars* represent ± SEM (*$P < 0.05$, **$P < 0.01$, ***P < 0.001).

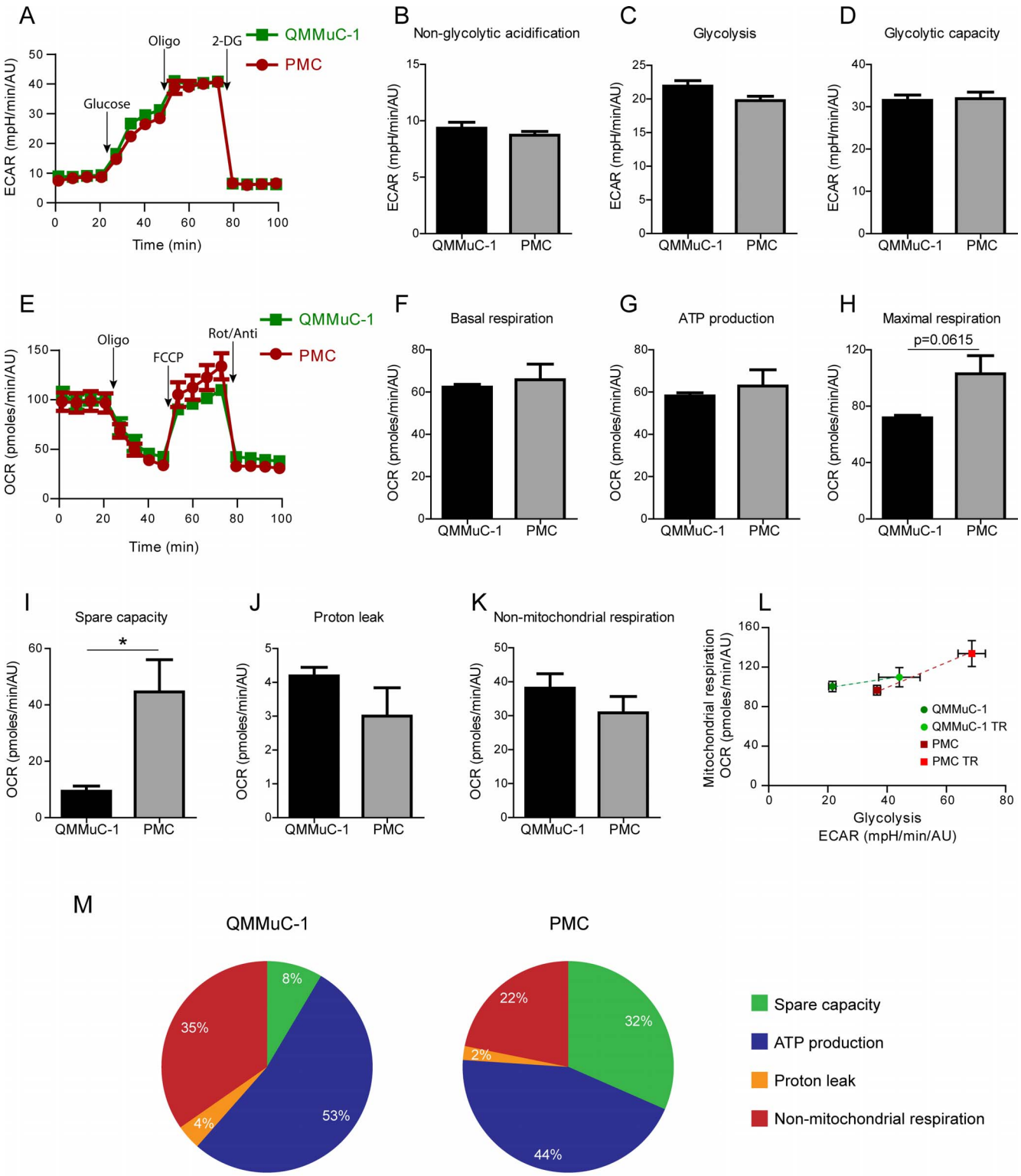

Figure 5. QMMuC-1 has a similar bioenergetic profile to PMC. (**A**) Glycolysis stress assay demonstrated similar profiles between QMMuC-1 (*green*) and PMC (*red*). (**B**) Nonglycolytic acidification rate, (**C**) glycolysis, and (**D**) glycolytic capacity are similar between the two cell types. (**E**) Basal OCR levels are similar between PMC and QMMuC-1. PMC show a greater increase in OCR after FCCP treatment compared to QMMuC-1. (**F**) Mitochondrial basal respiration and (**G**) ATP production are comparable between the two cell types. (**H**) Maximal respiration and (**I**) spare capacity are higher in PMC than QMMuC-1. (**J**) Proton leak and (**K**) nonmitochondrial respiration are similar between the two. (**L**) Phenotypic analysis of QMMuC-1 and PMC showing the relative mitochondrial respiration and glycolysis at the basal level and after oligomycin and FCCP treatment (TR) in the Mito Stress assay. (**M**) Pie charts showing the relative percentage of oxygen consumption used by nonmitochondrial respiration, proton leak, ATP production, and spare capacity in the two cell types. 2-DG: 2-Deoxy-D-glucose, oligo: oligomycin, Rot/Anti: rotenone and antimycin A. $n = 5$. *Error bars* represent ± SEM (*$P < 0.05$).

Investigative Ophthalmology & Visual Science

confirming the lower maximal metabolic capacity of QMMuC-1 compared with PMC.

Further analysis of oxygen consumption in QMMuC-1 cells revealed that 53% of the O_2 was used by mitochondria to produce ATP, whereas, 4% and 35% of the usage were due to proton leakage and nonmitochondrial-related activities in QMMuC-1 cells, respectively (Fig. 5M). That leaves only 8% of oxygen for spare capacity in QMMuC-1 cells as compared with 32% in PMC cells (Fig. 5M), which may explain the lower spare respiratory capacity of QMMuC-1 cells.

Discussion

In this study, we report a spontaneously immortalized murine Müller cell line, QMMuC-1, which has been cultured for over 60 passages.

The morphology and phenotype of QMMuC-1 resemble those of primary Müller glial cultures, despite numerous rounds of passaging. Aside from the characteristic Müller glial markers (GFAP, GS, α-SMA, and Vim), QMMuC-1 cells also express Kir4.1 and Aqp4, which are key molecules used by Müller glia to regulate potassium and water homeostasis in the retina, respectively. Müller glia are known to release various cytokines and neurotrophic factors. Compared with PMC, QMMuC-1 express higher levels of Ccl2 and VEGFA, but lower levels of IL-6 and GFAP. As for neurotrophic factors, QMMuC-1 cells express comparable levels of CNTF, but lower levels of BDNF and IGF1 compared with PMC. Interestingly, NTF3 was not detected in QMMuC-1 cells although it was detected at significant levels in PMC. These results suggest that QMMuC-1 may represent a distinct subset of Müller glia.[30]

One of the major challenges with primary Müller glial culture is the contamination by retinal neurons and other glial cells.[14] The lack of Cone arrestin (marker for cone photoreceptors) and Calb1 (marker for amacrine cell) expression in the earlier passage of PMC suggested the cell culture system was not contaminated by other neuronal cells. Although, astrocytes also express GFAP and α-SMA, they do not express CRALBP (which is a Müller glia–specific marker).[18] IL-33, a member of the IL-1 family, is constitutively expressed in the nuclei of various cell types including endothelial cells and epithelial cells.[31] In the eye, IL-33 is expressed in Müller glia, a small number of amacrine cells[31,32] and also at low levels in ganglion and RPE cells[32,33] and expression of this cytokine was confirmed in the nuclei of both QMMuC-1 (Fig. 2K) and PMC (Fig. 1F). The positive staining of CRALBP and IL-33 suggests that QMMuC-1 are Müller glia and not astrocytes.

Glutamate is a major excitatory neurotransmitter in the visual pathway. Müller glia are the main cell type involved in clearing excessive glutamate in the retina, although other neuronal cells, such as photoreceptors, horizontal, and bipolar cells are also known to play a role.[5] Retinal neuronal cell death can occur at concentrations as low as 5 μM glutamate,[34] and therefore, Müller glia play a crucial neuroprotective role in the retina. Müller glia express specialized transporters to regulate extracellular glutamate levels with GLAST being one of the most important. In the present study, both glutamate and PDC (a selective glutamate transporter ligand) evoked ionic currents in QMMuC-1 cells similar to those recorded in PMC and those previously described in freshly isolated Müller glia.[21] Furthermore, GLAST was detected at the molecular (mRNA) level in these cells. Therefore, these findings suggest that QMMuC-1 cells possess glutamate regulatory mechanisms resembling those of Müller glia in vivo.

Müller glia display a high metabolic rate, which is related to their diverse functions. The detailed ATP-generating metabolism of Müller glia remains to be fully defined. Previous work has shown that in the presence of glucose and oxygen, cultured Müller glia generate ATP mainly by glycolysis.[35] After glucose deprivation and inhibition of mitochondria, ATP production was suppressed,[35] whereas inhibiting mitochondrial respiration using antimycin-A in the presence of glucose did not affect Müller cell (MIO-M1) viability.[36] Another study, however, showed that mitochondria are important for Müller glial function and disturbing mitochondria reduced glutamate uptake and cell survival.[37] We have found that both glycolysis and mitochondrial respiration were active in Müller glia. QMMuC-1 and PMC had similar levels of glycolysis and glycolytic capacity. In addition, basal mitochondrial respiration and ATP production were comparable between QMMuC-1 and PMC. Under aerobic conditions, ATP is mainly produced by mitochondrial oxidative phosphorylation in most cell types. It has been proposed that Müller glia may rely on the Tricarboxylic Acid (TCA) cycle to produce ATP.[38] Our Mito Stress assay showed that the OCR/ECAR ratio was significantly higher in QMMuC-1 (4.79 ± 0.49) when compared with PMC (2.85 ± 0.3). A higher OCR/ECAR ratio suggests increased mitochondrial respiration in relation to glycolysis. Therefore, our data suggest that QMMuC-1 depend more on mitochondrial respiration for ATP generation than PMC. Interestingly, the spare respiratory capacity was significantly lower in QMMuC-1 cells compared with PMC, suggesting that the immortalized cell line has lower capacity to support additional energy demands.

Conclusions

In summary, the murine QMMuC-1 cell line is morphologically and phenotypically representative of PMC. The cells also express various cytokines and neurotrophic factors, and respond to glutamate stimulation. However, the cell line has its own metabolic profile and is fueled more by mitochondrial respiration compared to primary Müller cells. Compared with other Müller cell lines, QMMuC-1 has a number of advantages. First, it originates from a C57BL/6J mouse, a common laboratory mouse widely used to study retinal diseases. Data collected from this cell line will therefore be readily applicable for in vivo verification in animal models. Second, the QMMuC-1 cells have a relatively mature phenotype and are stable in normal culture conditions, and thus can be used for a variety of Müller cell–related studies. Third, they grow rapidly and can maintain as monolayer for a sustained period of time. This cell line, therefore, is suitable to model chronic conditions. Taken together, our data suggest that QMMuC-1 could be a useful tool for studying the physiology and pathophysiology of Müller glia.

Acknowledgments

Supported by grants from Fight for Sight (1574/1575; London, UK), National Eye Research Centre (SCIAD076; Bristol, UK), and Diabetes UK (13/0004729; London, UK).

Disclosure: **J. Augustine**, None; **S. Pavlou**, None; **M. O'Hare**, None; **K. Harkin**, None; **A. Stitt**, None; **T. Curtis**, None; **H. Xu**, None; **M. Chen**, None

References

1. Duh EJ, Sun JK, Stitt AW. Diabetic retinopathy: current understanding, mechanisms, and treatment strategies. *JCI Insight*. 2017;2e93751.
2. Vecino E, Rodriguez FD, Ruzafa N, Pereiro X, Sharma SC. Glia-neuron interactions in the mammalian retina. *Prog Retin Eye Res*. 2016;51:1–40.

3. Reichenbach A, Bringmann A. New functions of Müller cells. *Glia*. 2013;61:651–678.
4. Puro DG, Roberge F, Chan CC. Retinal glial cell proliferation and ion channels: a possible link. *Invest Ophthalmol Vis Sci*. 1989;30:521–529.
5. Bringmann A, Grosche A, Pannicke T, Reichenbach A. GABA and glutamate uptake and metabolism in retinal glial (Müller) cells. *Front Endocrinol (Lausanne)*. 2013;4:48.
6. Labin AM, Ribak EN. Retinal glial cells enhance human vision acuity. *Phys Rev Lett*. 2010;104:158102.
7. Franze K, Grosche J, Skatchkov SN, et al. Müller cells are living optical fibers in the vertebrate retina. *Proc Natl Acad Sci U S A*. 2007;104:8287–8292.
8. Nagashima M, Barthel LK, Raymond PA. A self-renewing division of zebrafish Müller glial cells generates neuronal progenitors that require N-cadherin to regenerate retinal neurons. *Development*. 2013;140:4510–4521.
9. Fischer AJ, Reh TA. Müller glia are a potential source of neural regeneration in the postnatal chicken retina. *Nat Neurosci*. 2001;4:247–252.
10. Roesch K, Jadhav AP, Trimarchi JM, et al. The transcriptome of retinal Müller glial cells. *J Comp Neurol*. 2008;509:225–238.
11. Lawrence JM, Singhal S, Bhatia B, et al. MIO-M1 cells and similar Müller glial cell lines derived from adult human retina exhibit neural stem cell characteristics. *Stem Cells*. 2007;25:2033–2043.
12. Das AV, Mallya KB, Zhao X, et al. Neural stem cell properties of Müller glia in the mammalian retina: regulation by notch and wnt signaling. *Dev Biol*. 2006;299:283–302.
13. Goldman D. Müller glial cell reprogramming and retina regeneration. *Nat Rev Neurosci*. 2014;15:431–442.
14. Sarthy VP, Brodjian SJ, Dutt K, Kennedy BN, French RP, Crabb JW. Establishment and characterization of a retinal Müller cell line. *Invest Ophthalmol Vis Sci*. 1998;39:212–216.
15. Otteson DC, Phillips MJ. A conditional immortalized mouse Müller glial cell line expressing glial and retinal stem cell genes. *Invest Ophthalmol Vis Sci*. 2010;51:5991–6000.
16. Tomi M, Funaki T, Abukawa H, et al. Expression and regulation of L-cystine transporter, system xc-, in the newly developed rat retinal Müller cell line (TR-MUL). *Glia*. 2003;43:208–217.
17. Lupien CB, Salesse C. Characterization of two spontaneously generated human Müller cell lines from donors with type 1 and type 2 diabetes. *Invest Ophthalmol Vis Sci*. 2007;48:874–880.
18. Limb GA, Salt TE, Munro PM, Moss SE, Khaw PT. In vitro characterization of a spontaneously immortalized human Müller cell line (MIO-M1). *Invest Ophthalmol Vis Sci*. 2002;43:864–869.
19. Dun Y, Mysona B, Itagaki S, Martin-Studdard A, Ganapathy V, Smith SB. Functional and molecular analysis of D-serine transport in retinal Müller cells. *Exp Eye Res*. 2007;84:191–199.
20. Phillips MJ, Otteson DC. Differential expression of neuronal genes in Müller glia in two- and three-dimensional cultures. *Invest Ophthalmol Vis Sci*. 2011;52:1439–1449.
21. Li Q, Puro DG. Diabetes-induced dysfunction of the glutamate transporter in retinal Müller cells. *Invest Ophthalmol Vis Sci*. 2002;43:3109–3116.
22. McDowell RE, McGahon MK, Augustine J, Chen M, McGeown JG, Curtis TM. Diabetes impairs the aldehyde detoxifying capacity of the retina. *Invest Ophthalmol Vis Sci*. 2016;57:4762–4771.
23. Kumar A, Shamsuddin N. Retinal Müller glia initiate innate response to infectious stimuli via toll-like receptor signaling. *PLoS One*. 2012;7:e29830.
24. Chen M, Muckersie E, Robertson M, Fraczek M, Forrester JV, Xu H. Characterization of a spontaneous mouse retinal pigment epithelial cell line B6-RPE07. *Invest Ophthalmol Vis Sci*. 2008;49:3699–3706.
25. Chen M, Rajapakse D, Fraczek M, Luo C, Forrester JV, Xu H. Retinal pigment epithelial cell multinucleation in the aging eye - a mechanism to repair damage and maintain homoeostasis. *Aging Cell*. 2016;15:436–445.
26. Pavlou S, Wang L, Xu H, Chen M. Higher phagocytic activity of thioglycollate-elicited peritoneal macrophages is related to metabolic status of the cells. *J Inflamm (Lond)*. 2017;14:4.
27. Puro DG, Yuan JP, Sucher NJ. Activation of NMDA receptor-channels in human retinal Müller glial cells inhibits inward-rectifying potassium currents. *Vis Neurosci*. 1996;13:319–326.
28. Kusaka S, Kapousta-Bruneau NV, Puro DG. Plasma-induced changes in the physiology of mammalian retinal glial cells: role of glutamate. *Glia*. 1999;25:205–215.
29. Bridges RJ, Stanley MS, Anderson MW, Cotman CW, Chamberlin AR. Conformationally defined neurotransmitter analogues. Selective inhibition of glutamate uptake by one pyrrolidine-2,4-dicarboxylate diastereomer. *J Med Chem*. 1991;34:717–725.
30. Hamon A, Roger JE, Yang XJ, Perron M. Müller glial cell-dependent regeneration of the neural retina: an overview across vertebrate model systems. *Dev Dyn*. 2016;245:727–738.
31. Pichery M, Mirey E, Mercier P, et al. Endogenous IL-33 is highly expressed in mouse epithelial barrier tissues, lymphoid organs, brain, embryos, and inflamed tissues: in situ analysis using a novel il-33-LacZ gene trap reporter strain. *J Immunol*. 2012;188:3488–3495.
32. Xi H, Katschke KJ Jr, Li Y, et al. IL-33 amplifies an innate immune response in the degenerating retina. *J Exp Med*. 2016;213:189–207.
33. Barbour M, Allan D, Xu H, et al. IL-33 attenuates the development of experimental autoimmune uveitis. *Eur J Immunol*. 2014;44:3320–3329.
34. Lipton SA, Rosenberg PA. Excitatory amino acids as a final common pathway for neurologic disorders. *N Engl J Med*. 1994;330:613–622.
35. Winkler BS, Arnold MJ, Brassell MA, Puro DG. Energy metabolism in human retinal Müller cells. *Invest Ophthalmol Vis Sci*. 2000;41:3183–3190.
36. Skytt DM, Toft-Kehler AK, Braendstrup CT, et al. Glia-neuron interactions in the retina can be studied in cocultures of Müller cells and retinal ganglion cells. *Biomed Res Int*. 2016;2016:1087647.
37. Vohra R, Gurubaran IS, Henriksen U, et al. Disturbed mitochondrial function restricts glutamate uptake in the human Müller glia cell line, MIO-M1. *Mitochondrion*. 2017;36:52–59.
38. Rueda EM, Johnson JE Jr, Giddabasappa A, et al. The cellular and compartmental profile of mouse retinal glycolysis, tricarboxylic acid cycle, oxidative phosphorylation, and ~P transferring kinases. *Mol Vis*. 2016;22:847–885.

Investigative Ophthalmology & Visual Science